Journal of Molecular Liquids 359 (2022) 119300

Contents lists available at ScienceDirect

Journal of Molecular Liquids

journal homepage: www.elsevier.com/locate/molliq

May sediments affect the inhibiting properties of NaCl on CH_4 and CO_2 hydrates formation? an experimental report

Rita Giovannetti [a,*], Alberto Maria Gambelli [b], Beatrice Castellani [b], Andrea Rossi [a], Marco Minicucci [c], Marco Zannotti [a], Yan Li [d,e], Federico Rossi [b]

[a] School of Science and Technology, Chemistry Division, ChIP Research Center, University of Camerino, Camerino, 62032, Italy
[b] Engineering Department, University of Perugia, Via G. Duranti 93, Perugia, 06125, Italy
[c] School of Science and Technology, Physics Division, University of Camerino, Camerino, 62032, Italy
[d] CAS Key Laboratory of Experimental Study under Deep-sea Extreme Conditions, Institute of Deep–sea Science and Engineering, Chinese Academy of Sciences, Sanya, Hainan 572000, China
[e] University of Chinese Academy of Sciences, Beijing 100049, China

ARTICLE INFO

Article history:
Received 7 February 2022
Revised 29 March 2022
Accepted 28 April 2022
Available online 4 May 2022

Keywords:
CO_2 gas hydrates
Natural chemical inhibitors
Temperature analysis
Raman OH-stretching vibrations
SEM

ABSTRACT

The equilibria of methane and carbon dioxide clathrate hydrates were measured in presence of a pure-quartz porous sand, with and without NaCl. Two different salt concentrations were tested: 0.030 and 0.037 wt%. Results were compared with phase equilibrium data already present in literature for these species. Despite salt, the porous medium was found to promote the process, mainly for the increased surface/volume ratio and for the improved heat transfer. In presence of salt, sand affected the process differently as a function of temperature: at values higher than 3 – 5 °C, it promoted the process, while for values lower than this range, but still greater than the ice-point, it acted as an inhibitor. However, these results can be considered true only for temperatures above the ice point.

Due to similarity of ice water with clathrate hydrates, Raman microscale measurements were performed to gather information about the influence of sediments, salt, and temperature on OH-stretching vibrations of water. The obtained results allowed to clarify how the addition of NaCl, and or sediments to liquid water, under different temperature conditions (15 °C and −15 °C), influenced the water hydrogen bonds. Specifically, the changes of OH-stretching vibrations, when correlated with the NaCl concentrations, demonstrated that the presence of sediments partially inhibited the salt effects in the ice water probably due to hydrophilic interactions with the silanol groups of sediments. SEM measurements showed morphological information on sediments and on ice in different experimental conditions.

1. Introduction

Natural gas hydrates are ice-like caged crystalline compounds composed of water and natural gas under suitable conditions of temperature, pressure, and gas saturation salinity, in which water molecules as the primary body can capture the guest gas molecules through the cavity built by hydrogen bonding. Natural gas molecules found in hydrates nowadays include hydrocarbon gases [1] and non-hydrocarbon gases (carbon dioxide, hydrogen sulfide, nitrogen, and so on). An empty hydrate can be considered as unstable ice: it becomes a stable gas hydrate when the pores are filled with single or mixed gas guest molecules. The conditions for hydrate formation differ depending on the type of guest molecules, and the three most common structures of hydrate crystal generated: cubic structure I, cubic structure II, and hexagonal structure H [2,3]. Hydrate former composition and thermodynamic conditions determine which structure can be formed.

It has been widely reported that natural gas hydrates have a high capacity to store gas, and one volume of natural gas hydrate can store 160–180 times the volume of gas. The main component of natural gas hydrates present in nature is methane (more than 90%) [4,5]. The stability of natural gas hydrates in nature depends on temperature, pressure, and the interrelationship between gas–water components. These factors limit the distribution of hydrates to the shallow part of the lithosphere, up to 2000 m below the surface, such as a permafrost region and an outer continental margin marine setting [6,7]. 99% of global hydrates are distributed in the

* Corresponding author.
E-mail address: rita.giovannetti@unicam.it (R. Giovannetti).

https://doi.org/10.1016/j.molliq.2022.119300
0167-7322/

Gas Hydrate Stability Zone (GHSZ) on the seafloor, which is influenced by geothermal gradients, pressure effects and actual gas concentrations in the environment, and the areas of stable hydrate presence in nature are mainly concentrated in the low-temperature and high-pressure zones [5,8,9]. Since the majority of naturally produced hydrates are distributed as solids in porous sediments on the seafloor, porous media are characterized by large specific surface area and prominent interfacial phenomena (manifested by strong interfacial tension and capillary coalescence). Gradually, the research on the phase equilibrium of gas hydrate was carried out by artificial porous media such as porous silica and porous glass [10–14], and the laboratory measurement and theoretical prediction models of natural sediments (clay, silt, gravel, etc.) containing gas hydrate were carried out [15].

Pure water/seawater is an inevitable element in the formation of hydrates, and its composition and concentration are also important factors affetting the hydrate equilibrium. The salt ions widely present in seawater are Na^+, Cl^-, and Mg^{2+}, Ca^{2+}, SO_4^{2-}, etc. The effect of various electrolytes on hydrate formation and dissociation has been studied extensively in previous literatures [16–18]. All these publications demonstrate how the presence of salt dissolved in water, acting as thermodynamic inhibitor, increases the hydrate equilibrium pressure and/or decreases the equilibrium temperature. In addition, what is widely known, is that electrolytes in seawater do not enter the hydrate structure. Thus, the desalination technology could be performed based on the hydrate formation and decomposition [19,20]. For the development of advancement of these novel technologies, extensive efforts have gone into understanding thermophysical properties and characteristics of CH_4 and CO_2 hydrates, such as CO_2 separation [21] and capture [22,23], the recovery of CH_4 from natural gas hydrates [24,25], and the storage and safe transportation of CH_4 using hydrates [26,27].

Water has many unique properties with important functions in many chemical reactions in natural systems. The water molecule has both double-donor and double-acceptor hydrogen-bond functionality that permits to obtain a wide range of flexibility without substantial loss of hydrogen-bonding energy. Hydrogen bond network is therefore not static due to the formation and breaking of hydrogen bonds that makes possible many of the processes that occur in water. A variety of parameters such as temperature, pressure and dissolved ions promote structural changes on water molecules with cooperative effects related to hydrogen bonds. For this, it is difficult to define the hydrogen-bond structure of an assembly of water molecules in the absence of precise information about the location of the hydrogen atoms and the dynamics of their motion [28,29].

Salts present in water act as thermodynamic inhibitors of gas hydrates, by disturbing the hydrogen bond network before the hydrate formation [30] with the consequent shift of equilibrium curve to lower temperature and higher pressure [31]. This effect is related to competition between coulombic and hydrogen bond forces related to water - salt and water-water respectively [32]. A decrease in the solubility of guest molecules occurs as the secondary effect of this clustering by "salting-out." The result of both effects is that more subcooling is necessary to overcome the structural changes necessary to obtain the hydrate formation [32].

Methane is the predominant gas in natural gas hydrates, and the hydrates that occur naturally or cause blockages in pipelines are also predominantly methane hydrates. Since Hammerschmidt discovered natural gas hydrates blockages in the natural gas transmission pipelines in 1934 [33], research on the phase behavior and on the characteristics of gas hydrates were promoted. Deaton et al. proposed the inhibition of hydrates [34], and de Roo et al. took salinity into account and systematically studied the equilibrium temperature and pressure conditions of methane hydrate phases in the CH_4-H_2O-NaCl ternary system [35]. Subsequently, involved various salt ions (Cl^-, Na^+, Mg^{2+}, SO_4^{2-}, Ca^{2+}) and transition metals (Fe, Mn, Cu, Co, Ni, etc.) in groundwater, scholars have studied more extensively the inhibition of methane hydrate by various salt ions, and basically determined the degree of inhibition of methane hydrate by various ions [36,37]. Due to the requirement for hydrate reservoir replacement [24] and the greenhouse environmental influence of CO_2, as well as the gradual discovery of high CO_2-containing gas reservoirs, research on CO_2 hydrate inhibitors is gradually being conducted. Vlahakis et al. released the phase equilibrium data of carbon dioxide hydrate in NaCl solution [38]; Zha et al. investigated the effect of NaCl-$MgCl_2$ mixed solution on the phase equilibrium of carbon dioxide hydrate [39]; Sun et al. studied the phase equilibrium of CO_2 hydrate under different conditions with NaCl solutions, seafloor pore water, and quartz sand + NaCl solution to simulate the storage of CO_2 hydrate in the ocean; additionally demonstrated that the decrease in phase equilibrium temperature of CO_2 hydrate in NaCl solution is mainly caused by Cl^- ions [40]. Numerous experimental and simulation results show that the phase equilibrium conditions of gas hydrate in the presence of electrolyte solution shift toward higher pressure and lower temperature [22,37,41–44].

Currently studies on natural gas hydrate in simulated reservoir conditions aim to approach to the production (decomposition) of hydrates. The most typical experimental design for examining hydrate production decomposing is to use an autoclave to generate huge hydrates, or to place some sands, quartz, core powder, or other similar materials in a reactor to generate a porous media environment [43,45,46]. Pore diameters in the porous media influence the hydrate formation and dissociation process. Anderson et al. [47,48] investigated extensively this issue and discovered that the size of the porous medium has a comparable inhibitory effect on the hydrate production process as the thermodynamic inhibiting agent (inorganic salt). However, the presence of salts in porous media impacted the kinetics of CH_4 hydrate formation, resulting in a drop in CH_4 hydrate production and in a change in the gas absorption curve, with the hydrates dissociating at a slower rate in seawater than in pure water [46]. Kang et al. [49] revealed that when porous water contents in silica gel are employed to create the gas hydrate, a greater conversion yield may be reached in a short amount of time without mechanical agitation. As a result, from a kinetic standpoint, the use of porous medium may offer certain advantages. However, it was also noted that in some literatures, the sands served as the inhibitor for decreasing water activity in silica gel pores [49]. Handa and Stupin [50] were the first to explore the influence of porous media on the equilibrium pressures of CH_4 and C_3H_8 hydrates, demonstrating that the equilibrium pressures of the corresponding gas hydrates in silica gel holes were greater than those of bulk hydrates.

There are several difficulties involved with the hydrate technique of CO_2 storage in porous material under seabed conditions. Mass transfer is a primary constraint that influences CO_2 storage capacity during hydrate formation, whereas temperature change within porous sediments impacts the hydrate dissociation process, affecting the thermal stability of the hydrates [51]. As a result, it is critical to perform research on the kinetic and stability of CO_2 hydrates in porous media [52]. Chong et al. [53] investigated the influence of NaCl on the kinetics of hydrate formation and dissociation in porous media and NaCl showed a strong kinetic inhibitory impact on hydrate formation, resulting in decreasing water conversion to hydrates, a slower formation rate, and a longer time to achieve a plateau for methane hydrate production [54]. Kinetic experiments of CO_2 hydrate formation in silica sand indicated that the induction of time for hydrate in seawater was lower than that of pure water, and silica sand with sea water provided an optimum environment for efficient hydrate formation [55]. It was also

shown that the optimal size of silica sand for CO_2 hydrate formation was 0.46 mm (compare to 0.16 mm and 0.92 mm). Yang et al [54] conducted experiments and revealed the evidence of thermodynamic inhibition other than kinetics inhibition of CO2 hydrate formation in porous media with salts.

Therefore, the effect of porous media such as silica sand may differ with the specific experimental conditions, porosity, and gravel size. On the one hand, holes increase the capillary forces that must be resist during the hydrate formation; the presence of porous media acts as a thermodynamic inhibitor to the formation of hydrates. In addition, the porous media, provides more nucleation sites for hydrates and enhances mass transfer due to its increased surface area and lower surface tension. At this point, the porous medium acts as a kinetic promoter that reduces the induction time.

Raman spectroscopy is a powerful technique for the investigation of the molecular structure and appropriate for the analysis of water, aqueous solutions, and its solid phases. Raman spectrum of water can be divided into three zones; the first, below 400 cm^{-1}, is due to translational/vibrational bands, the second at about 1600 cm^{-1} is related to OH–bending bands, and the third, the most intense, is in the range 3000–4000 cm^{-1} and regards the OH–stretching (OHs) bands. These bands permit the study of parameters affecting the water hydrogen bonds, by the modifications of the inter-molecular coupling of symmetric and asymmetric OH-stretching vibrations, giving therefore information about local structures and dynamic properties of water, aqueous solutions, and its phase. The Raman OHs band profile related to liquid water consists of three main components indicating multiple, single, and non-bond hydrogen bonding [56–58].

Due to the actual conditions of hydrate presence and seawater composition, chloride solutions can be used to simulate sea water and study the decomposition conditions of hydrates for a better understand of the boundary conditions of the hydrate stability. However, there was the limited description of the three-phase equilibrium conditions that coexist with seawater [59,60].

The ice water presents similarity with clathrate hydrates [61] and for this, in this study, for microscale measurements, we have selected the ice water as a model to gather information about the influence of sediments, salt and temperature on hydrates formation. First, SEM measurements were performed to obtain morphological information on sediments and ice. Successively we have investigated, by Raman spectroscopy, the water OH-stretching vibrations in the liquid and in the ice water and correlated the obtained results, regarding the modification induced by sodium chloride, sediments, and temperature, in different experimental conditions.

Moreover, the hydrate dissociation/formation conditions of methane and carbon dioxide, in the presence of pure water, 0.030 and 0.037 wt% (wt%) of NaCl solutions, were experimentally investigated respectively. We conducted experiments in solutions with and without sand in a lab-scaled reactor. In order to observe and assess the inhibitor/promoter differences, the equilibrium curves of methane and carbon dioxide between literatures and experiments were compared for each salinity concentration in the temperature range of 0 – 8 °C. Results were then compared with data present in literature and related to the same typology of experiments carried out without sand. The present comparison proved that the presence of a porous medium generally promotes the hydrates formation process, as expected. Moreover, sand grains were also found to counteract the inhibiting effect of salt molecules, thus favoring hydrates formation at milder conditions than those described in the literature in the presence of similar concentrations of sodium chloride but without sand.

All the results showed that, by observing the influence of salt and sediments from two different perspectives (microscopic measurements on ice and macroscopic measurements on gas hydrates), the hydrates formation process was favored by the porous medium which reduced the effect of the salt.

2. Methods

The investigation presented in this paper consists of two different approaches, microscopic and macroscopic, which are integrated to show how porous media and salt affect the hydrate formation process. In this paragraph, materials and methods concerning the two sets of measurements are presented.

2.1. Measure of micro-scale properties

2.1.1. Samples preparation

The materials used for the experiments were NaCl (Aldrich), ultrapure water (conductivity 0,18 μS/cm) obtained by Advantage A10 Millipore instrument (Milli-Q water). Aqueous solutions of different NaCl concentrations (from 0 to 70 g/l) were prepared. All the reagents were of analytical grade without further purification. The porous sediments used for experiments is the same previously described in Section 3.1.2.

2.1.2. Morphological study by SEM

Field Emission Scanning Electron Microscopy (FE-SEM, Sigma 300, Zeiss) operating at 7.0 kV, equipped with Energy Dispersive X-ray spectroscopy (EDX, Quantax, EDS, Bruker), was used to obtain morphological information of pure water and NaCl solution in the presence of sediments in the ice phase.

We conducted the low-temperature SEM experiments at the temperature of − 15 °C by using a special device temperature-controlled (Coolstage by Seben). This device consists of a single stage Peltier device, onto which a thermally isolated specimen holder is mounted. The Coolstage assembly is installed onto the SEM stage using an adaptor plate specific to the microscope and cooling pipes and electrical wires connect to the SEM feedthrough flange. External components are a recirculating water chiller and power supply case. The temperature of the Coolstage head can be set in the range –30 °C to + 45 °C during operation under high vacuum and the device is integrated fully by the SEM control software. Images at T = -15 °C, have been collected by using the in-lens detector in order to obtain full information about the surface state of the sample.

2.1.3. Raman setup

Raman spectra were collected with a Micro-Raman setup (Fig. 1a) that consists of a Czerny-Turner spectrometer (iHR320 Horiba Scientific) equipped with 600 g/mm grating (resolution 7.0 cm^{-1}) and an open space microscope to accommodate a Linkam THMS600 cell for low/high temperature conditions (ranging from −195 °C to 600 °C).

The experiments were performed with a laser having an excitation wavelength of 532 nm (max power 50mW), the total acquisition time for each spectrum was 300 s and two were the working-temperatures: 15 °C and −15 °C. This Raman setup was based on a back-scattering configuration and allowed to collect the spectrum through an Olympus LMPLFLN50XBD long-distance objective (working distance of 10.6 mm). The backscattered radiation is collected by a Syncerity cooled CCD camera with 1024x226 pixels. To be able to carry out measurements on a larger sample volume and thus obtain more correct analytical measurements, a special metal copper sample holder has been designed and realized modifying the factory setup, with increased dimensions respect to that supplied by the instrument, as shown in Fig. 1b.

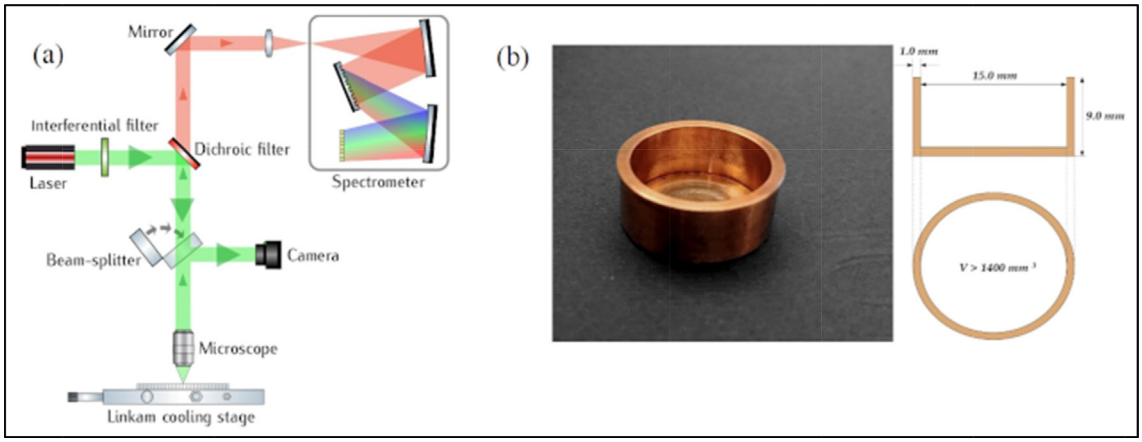

Fig. 1. Raman setup (a); sample holder (b).

2.2. Measure of macro-scale properties

2.2.1. Experimental apparatus

Gas hydrates were formed in a small-scale apparatus, designed to produce marine hydrate reservoirs. The formation environment consists of a 316SS reactor, having cylindrical volume (7.3 cm diameter and 22.1 cm height) equal to 949 cm^3. Two flanges close the reactor at the top and the bottom (see Fig. 2a). These flanges have a double function: ensuring high pressure tightness and providing high thermal capacity to the system, thus avoiding uncertainties due to external temperature variations.

The internal geometry of the reactor is more complicated than the external, due to the presence of channels, tiny tubes, and sensors. All these elements have been considered to define with accuracy the portion of volume free for the injection of raw materials and hydrates formation. All specifications are shown in Table 1.

The guest compound was injected from the bottom, to ensure more effective penetration of gaseous molecules into sand pores and between grains. The reactor has been inserted in a tank filled with a mixture of water and glycol. The tank is equipped with a double copper coil, directly connected to a chiller, model GC-LT. This vessel absorbs heat from the reactor (during hydrates formation) and releases it to the refrigerant fluid; conversely, during dissociation, it provides heat. In both cases, it intervenes when temperature variations occur and re-establishes the thermal balance in a shortened time period. At steady-state conditions, it works as a thermostatic bath for the system.

Table 1
Geometric and volume specifications of the reactor used for experiments.

Specification	Value	
Internal eight	22.1	cm
Depth from the edge	18.5	cm
Depth edge to the network	18.3	cm
Weld thickness	1.1	cm
Thickness from the edge	1	cm
Internal diameter	7.4	cm
Internal pipe volume	1	cm^3
Volume of intake pipes	19	cm^3
Gas volume from the high edge	90	cm^3
Total volume of free gas	109	cm^3
Internal reactor volume	949	cm^3

Fig. 2b shows a scheme of the assembled experimental apparatus. The choice to insert gas from the bottom also considered the presence of this bath. The gas cylinder is connected to the reactor via a little pipe, which passes through the bath before entering the reactor. Considering the very high surface/volume ratio of the pipe, such a system guarantees that, when gas enters inside, it has already assumed the same temperature of the formation environment. The temperature was measured with four Type K thermocouples, having class accuracy 1, and disposed at four different

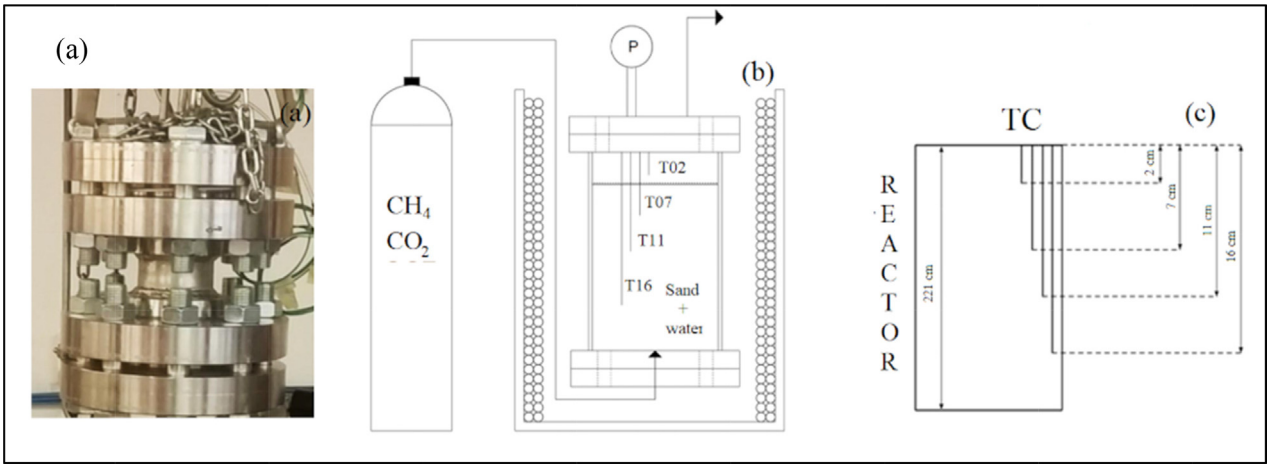

Fig. 2. Image of the lab-scale reactor used for hydrates formation and dissociation (a); scheme of the experimental apparatus (b); scheme of thermocouples positioning inside the reactor (c).

depths inside the reactor (respectively at 2, 7, 11 and 16 cm depth from the top). The disposition of thermocouples was established according to what was present in literature [55,62,63]. The positioning of thermocouples is described in Fig. 2c. The pressure was detected with a digital manometer, model MAN-SD, with class accuracy equal to ± 0.5% of full scale. All devices were finally connected to a data acquisition system, manufactured by National Instruments, and managed with LabView. A more detailed characterization of the present experimental apparatus is available elsewhere in the literature [64,65].

2.2.2. Materials.

Ultra-High-Purity (UHP) methane and carbon dioxide were used for hydrates production, with a purity degree respectively equal to 99.97% and 99.99%. The reactor was filled with 0.744 l of sand sediments. This latter compound consists of pure quartz spheres, with the diameter ranging from 200 to 500 μm, provided by the Geology Department of the University of Perugia. Sand porosity was measured with a porosimeter, model Thermo Scientific Pascal: it is equal to 34%. Spaces between sand grains were filled with 0.236 l of pure demineralized water. The remaining portion of volume was kept free for gas injection and is equal to 0.222 l. For tests with salt, NaCl was used in concentrations equal to 0.030 wt% and 0.037 wt%.

2.2.3. Gas hydrates preparation Methods.

The internal temperature of the reactor was firstly brought to 2 – 5 °C. Then the injection valve was slightly opened, and the gaseous compound fluxed inside the reactor. It mainly occupied the highest portion of the internal volume, where neither sand and water are present, and also diffused into sand pores, due to its porosity. Once the desired pressure was achieved, the injection valve was closed, and the reactor was kept free to operate in batch conditions. The contemporary occurrence of pressure and temperature conditions feasible for the process, led to an immediate formation of hydrates. Due to the entrapment of gaseous molecules in solid structures, pressure decreased continuously. The process was considered completed as soon as pressure approached a stable trend over time and stabilized.

The following dissociation phase was simply performed by switching off the chiller in order to generate a slow and gradual temperature increase inside the reactor. The associated increase in pressure, due to the release of gaseous molecules from water cages, allowed to define the equilibrium pressure–temperature curve for the system. Finally, the temperature used to describe experiments in the following section was calculated as average of temperatures measured by all thermocouples.

3. Results and discussions

3.1. Combined effect of sodium chloride and sand at temperatures below the ice-point.

3.1.1. Morphological study by SEM.

The morphology of sediment particles can play an important role in the interfacial interactions with water molecules and gas. In Fig. 3, the SEM images of sediments at different magnifications are reported. Fig. 3a evidences the size of sediments that is about 500 μm, Fig. 3b,c represent afar observations of the surface which highlights some irregularities, while Fig. 3d evidences a regular porosity of the sediment surface. When the sediments were added to pure water and the SEM measurements were conducted at −15 °C, the formed ice between the sediment particles showed an interesting structure. In fact, as visible in Fig. 4, the SEM images at different magnifications evidence that the ice shape is ramified around to punctiform water nanocrystals to form irregular structures. In Fig. 4b, to the right, is also evident the adhesion of the ice on the sediment surface that is magnified in Fig. 4c.

The addition of the NaCl solution to the sediments promotes the change of the ice structure between the sediment particles as evidenced in the SEM images of Fig. 5, where the different magnifications show that the ice is formed with regular structures. In particular, in Fig. 5a, the ice covers the particles surface of the sediments, in the Fig. 5b a magnification of about 5 times of this is evidenced, while, with higher magnification, crystals with very regular shape are highlights (Fig. 5 c,d,e).

3.1.2. Raman characterization

The O − H stretching bands (OHs) were selected in Raman characterization because these are the most intense bands that are closely related to the structure of water. A water molecule can form hydrogen bonds as a proton donor (D), proton acceptor (A) or combinations thereof, which can be of different types such as DDAA, DDA, DAA, DA, DD, AA, D and A in which the DD and AA structures are unfavorable while D and A can be present as dimers in supercritical water and in any case should not be considered at room temperature. Therefore, at room temperature, the Raman OH stretching vibration can be deconvolved into five sub-bands, DDAA-OH, DDA-OH, DAA-OH, DA-OH and free OH [66,67] (Fig. 6).

Fig. 6a shows the Raman spectrum of Milli-Q water at 15 °C with the results of deconvolution that describe the presence of five bands, the two main ones detected at 3400.3 cm^{-1} and 3215.5 cm^{-1}. When the Raman spectrum was measured at −15 °C and deconvolution is applied to Raman spectrum (Fig. 6b), a more intense peak related to the band detected at 3131.6 cm^{-1} appears while, on the contrary, the region below 3300 cm^{-1} clearly shows an increase of the intensity and therefore this band can be considered as an indicator of the ice. In this case, the water expansion and stability, which occurs in the ice phase, reduces the vibrational modes [68]. On the contrary, in the liquid phase, the asymmetric stretching is more intense due to flexible structure. In Table 2 all the bands are resumed.

NaCl solutions in which the salt dissociates into sodium and chloride ions are not Raman active. However, their effects in the solution can be evidenced indirectly by the observation of their influence on water vibrations and therefore in the modification of the water Raman spectrum. In this case, sodium and chloride ions orient towards the oxygen and hydrogen respectively. Only the interaction with chloride anions perturbs water molecules by breaking the hydrogen bonds, while sodium ion presents only a negligible effect [68]. The measurable effect on the water molecule, which can be attributed to modification of hydration shell of chloride, produces an increase of the amount of free O-H [69] with the related change of OHs bands.

In the liquid state of water, the effects of different dissolved NaCl concentrations in comparison with Milli- water on the relative OHs vibration bands of water at 15 °C and at atmospheric pressure, are described in Fig. 6c; as observed from the Figure, with increasing concentration of NaCl in the water, the band at around 3200 cm^{-1} (symmetric OHs) decreases in intensity while that at around 3400 cm^{-1} (asymmetric OHs) increases. The enhancement in NaCl concentration produced therefore a decrease in the number of hydrogen bonds, with a frequency shift, and an increase of the intensity of the asymmetric section of the OHs bands. No change in the trend is observed in the presence of sediments (Fig. 6d).

The Raman spectra of ice in the presence of NaCl shifted at higher frequencies according to the increase of NaCl concentration showing that the contribution of the region below 3300 cm^{-1} decreases (Fig. 6e) with the suppression of the related bands. These results indicate therefore that, in the ice state, the increase in NaCl concentration produced a decrease of symmetric OHs bands, with a

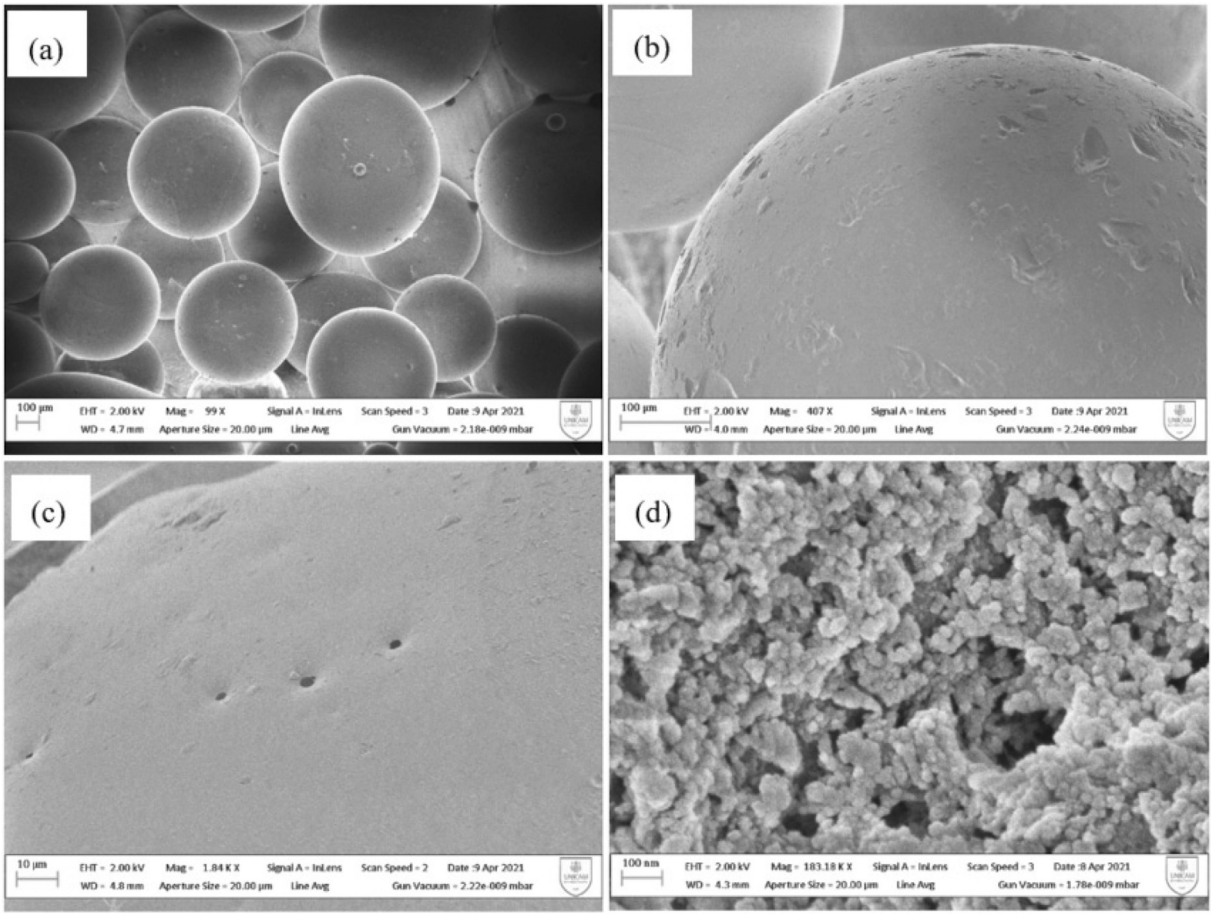

Fig. 3. SEM images showing the morphology of sediments surface at different magnifications.

frequency shift and an increase of the intensity of the asymmetric OHs bands; this effect is also detected in the presence of sediments (Fig. 6f).

The large polarizable chloride anions affect its propensity to the air/water interface thus influencing the free O-H groups differently [70,71]; this can be confirmed by the different frequency shifts of asymmetric OHs bands, from liquid and ice water at the same salinity conditions. In fact, as described of Fig. 6 (c-f) in the free O-H region of ice the observed shift is more affected by the increase of chloride anions.

To obtain information from all these results, the ratios between the areas of the symmetric and asymmetric bands were calculated in the range 3000–3600 cm^{-1} [69]. For this calculation, the isosbestic points were determined on the obtained spectra assuming that these points of frequency divide the spectra into two A and B regions that are associated with the symmetric and asymmetric OHs bands of water respectively; this concept is graphically described in Fig. 7 where isosbestic point at 3325 cm^{-1} is evidenced for the liquid phase of pure water.

The areas of the two regions were therefore measured in each experimental condition and the ratios of the corresponding integrated intensities of the two regions (B/A), that represent S_D concentration index [68,69,72], were correlated with the increase of NaCl concentration. Fig. 8a evidences the high correlation between S_D and NaCl concentration in the absence and in the presence of sediments at 15 °C also showing no particular differences in the two experimental conditions; these results demonstrate that, in the liquid state, the presence of sediments does not affect the symmetric and asymmetric OHs bands.

However, when the same calculation is applied in the ice state at −15 °C, differences in S_D concentration index were notified. In fact, two quasi-parallel straight lines are obtained (Fig. 8b), in which that in the presence of sediments is lowered the respect to the same in its absence.

In these experiments, the presence of sediments produced conditions comparable to those obtained by reducing the salt concentration; at example, the effect decreases by about 19% in the presence of 37 g/l of NaCl. In the case of sand, these results can be explained by considering that the water molecules, located on the silicate surface of sediments, can interact with these by intermolecular hydrogen bonds between water molecules and silanol groups as schematized in Fig. 8c; this interaction can be therefore in competition with that caused by the salt, limiting partially its effect [73].

The application of this method of data correlation, in the presence of different salt concentrations, can reflect therefore the changes in the physical and chemical properties of water molecules in the ice phase when in the presence of foreign substrate (sand in this case).

3.2. Gas hydrate formation in presence of sodium chloride and sand.

Gas hydrates were formed in the presence of sand and with different salt concentrations. For each guest compound considered (methane and carbon dioxide), three experiments were shown and described. The first of them was carried out in pure demineralized water, without any addition of salt, while the remaining two were carried out with a concentration of NaCl respectively equal to

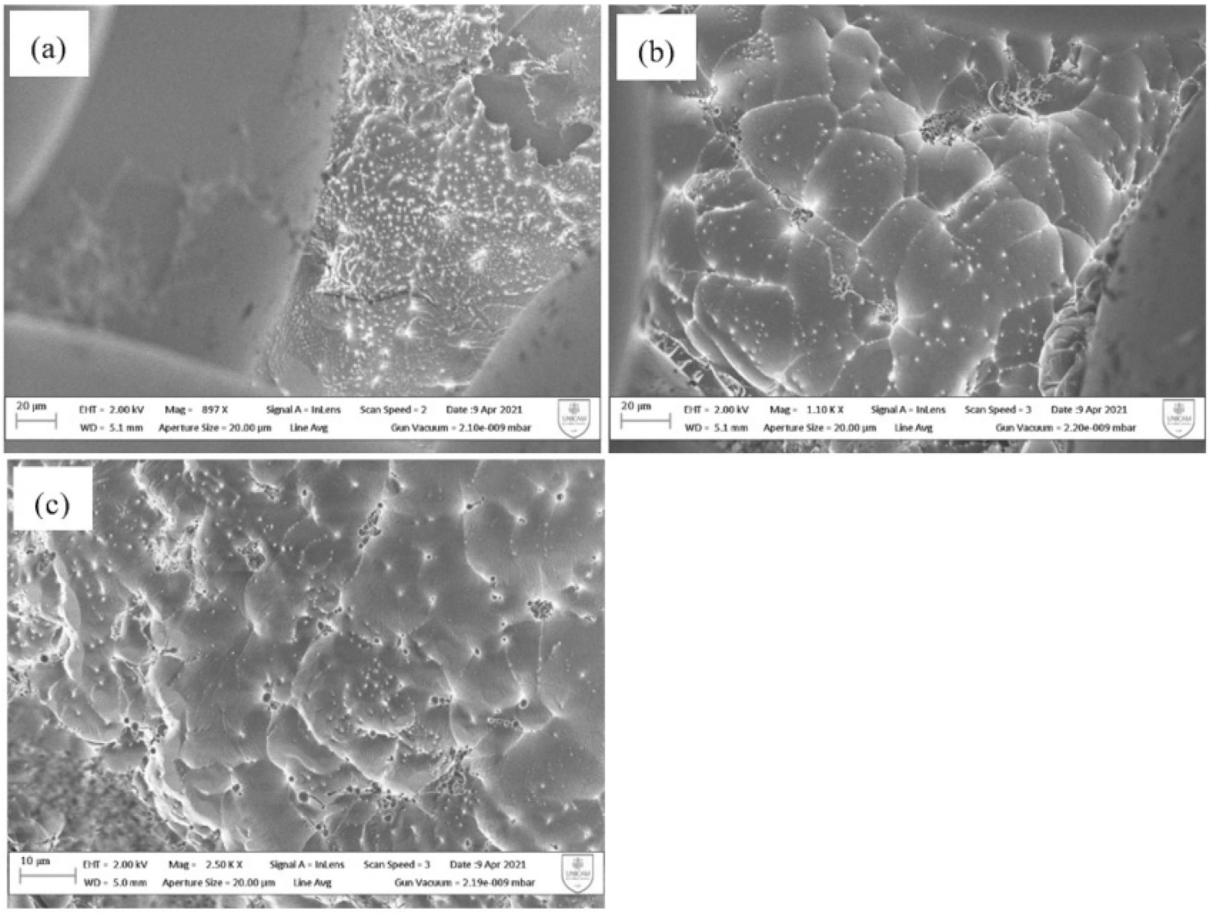

Fig. 4. SEM images showing the surface morphology of pure-ice water in presence of sediments at different magnifications.

0.030 wt% and 0.037 wt%. The different concentrations were selected in order to consider salinity degrees equal to those commonly measured in correspondence of marine hydrate reservoirs. Table 3 resumes the experiments carried out in this section. Experiments were performed according to what was asserted in Section 2.1.

3.2.1. Experiments carried out with methane as guest compound.

In Fig. 9, graphs a),b),c) show a comparison between methane hydrate dissociation p-T values, produced in lab experiments, with values found in literature, regarding the same sodium chloride concentrations but in the absence of sand. Fig. 9a, related to methane hydrates equilibrium in the absence of sodium chloride, clearly shows the promoting effect of sand. The experimental curves, carried out in the presence of the porous medium, are represented as a continuous line, that is visibly below the dotted line, produced with equilibrium values for methane hydrates in the absence of sand and directly taken from literature.

The promoting effect of sand in the hydrates formation is mainly due to the presence of grains, which ensure a more elevated surface/volume ratio, thus provide providing more potential nucleation sites per unit of volume for methane hydrates. Moreover, the presence of pores and cavities between grains promotes the formation of numerous secondary gas–liquid interfaces; this latter configuration was proved to be the most probable sites in which the reaction may start. In particular, three different hydrate crystals growth upon sand grains are possible: pore filling, cementation and supporting matrix; this explains why thermodynamic conditions, describing methane hydrates equilibrium, were milder in the presence of sand. However, controversial assumption can be found in literature, about the contribution on the process associated to the porous medium. For that reason, experimental studies focused on the process characterization (both formation and dissociation) in the presence of the porous media, mainly found in marine hydrate reservoirs, are needed [74]. Selim and colleagues performed a model to define the mass and heat transfer during CH4 hydrates dissociation and in presence of porous media [75] concluding that the heat transfer mechanism is mainly affected by the surrounding sediments. The phase equilibrium conditions for gas hydrates are defined during their dissociation. In presence of porous sand, the free water molecules will immediately produce an adherent layer on the surface of grains and will cause a reduction of the hydrate dissociation rate [76]. In addition, the sand also increased the heat transfer rate inside the reactor, due to its higher thermal conductivity, with a consequent increase of the hydrate dissociation rate. The heat transfer has crucial importance during hydrate formation because, as explained in literature, the production of heat during the initial nucleation phase can be abundant enough to inhibit the process and lowering the whole formation [46]. The entity of such aspect is clearly more pronounced if the process is carried out in a small volume. Thus, the presence of a pure quartz porous medium plays a key role in smoothing the peaks in temperature which naturally occur during hydrates formation. As a consequence, the time required to reach the thermal balance inside the reactor after temperature peaks is lowered.

Thus, the two profiles of Fig. 9a are parallel and the one referred to tests made with sand is shifted to milder thermodynamic conditions (lower pressures and higher temperatures). In particular, at

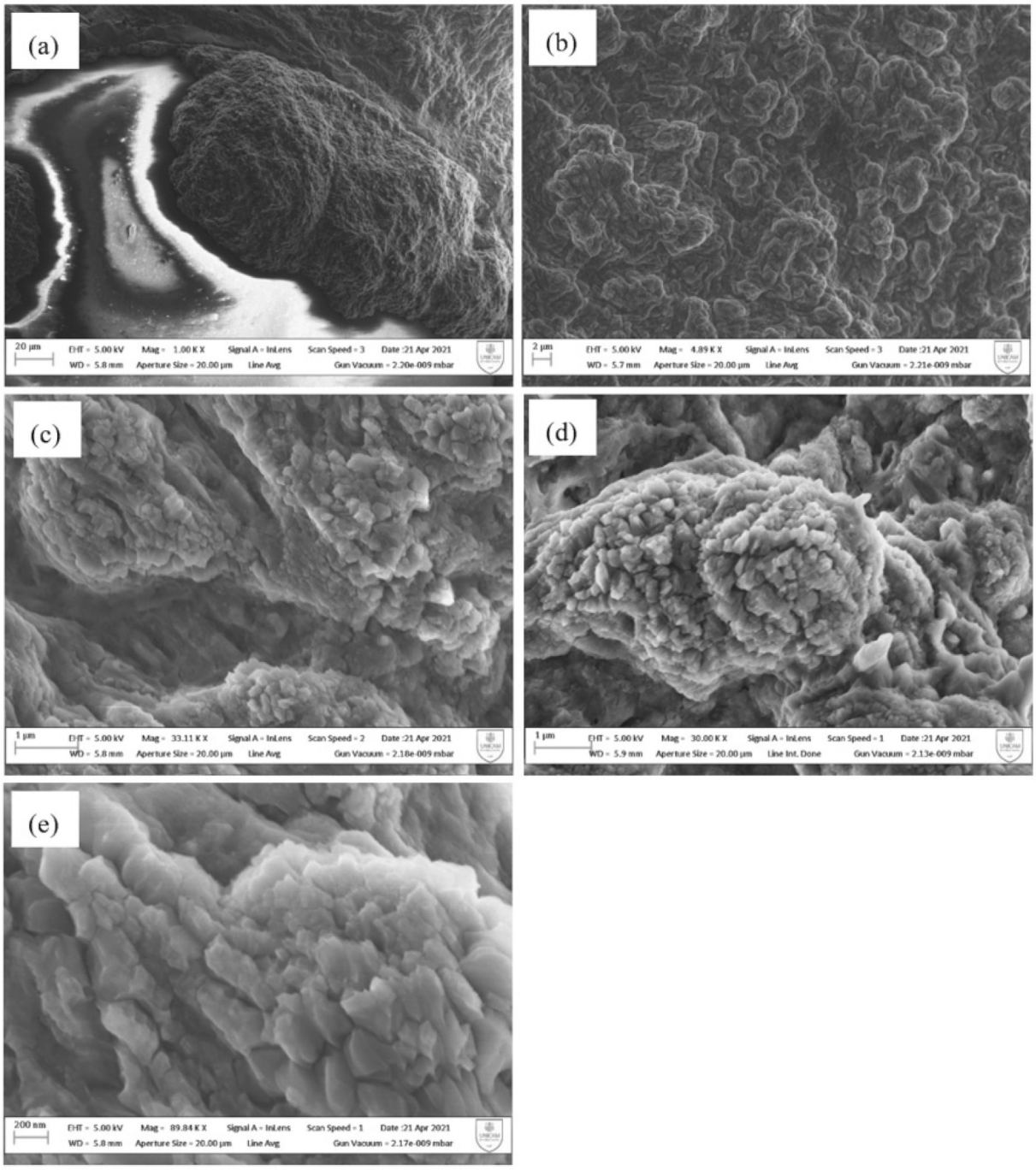

Fig. 5. SEM images showing the surface morphology of ice of NaCl solution (30 g/l) in presence of sediments.

the same pressure values, the formation temperature, in the presence of sand, is higher about 0.8 – 0.9 °C, while, at the same temperature, pressure is approximately 0.3 – 0.4 MPa lower.

In the presence of salt, the situation is completely different (Fig. 9 b, c). The two profiles are not parallel anymore and a point of intersection was observed at 3 °C (Fig. 9b) and at 5 °C (Fig. 9c). The profile in Fig. 9b describing the test made with 0.030 w NaCl, was compared with values of literature carried out with the same salt concentration and no sand. As far as Fig. 9c is concerned, p-T values with 0.037 w NaCl in absence of sand were not found in literature (values with similar concentrations were found only in the presence of sand). So, the comparison was made with p-T values produced in the presence of 0.050 w of NaCl. This could result in lower temperature value at the intersection point.

Moving on the right from the intersection point, the sand acted as promoter for the process; conversely, on the opposite side it acted as an inhibitor. In both cases, the entity of its promoting/inhibiting effect was found to be stronger with increasing/decreasing temperatures. This aspect confirms what emerged from the micro-scale analyses: the sand clearly varied the effect of sodium chloride on hydrate formation, by varying its interaction with water molecules and so affecting its inhibiting action. In accordance with micro-scale analyses, these experiments highlighted the presence of a strong relationship between the effect exercised by sand and temperature.

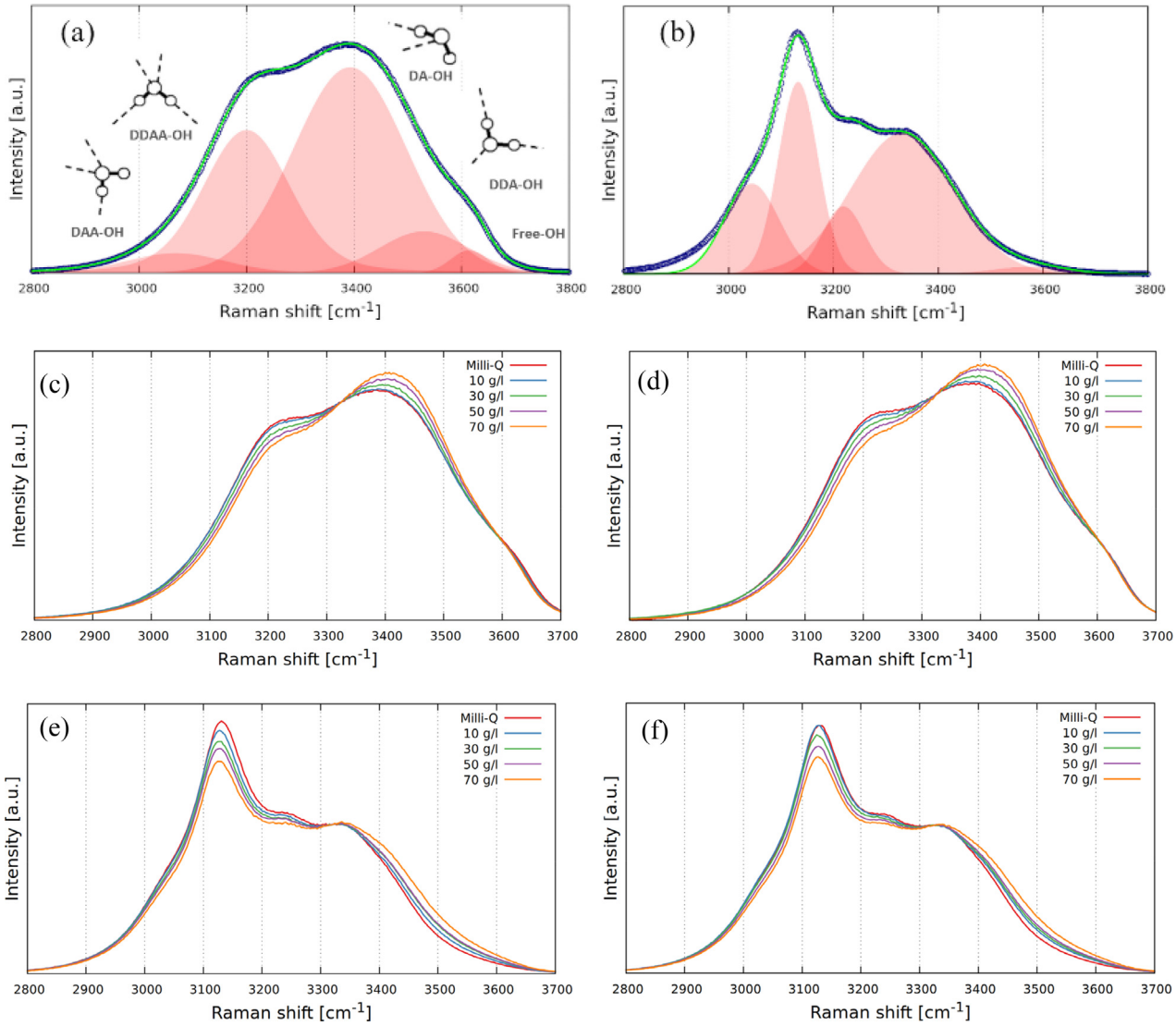

Fig. 6. Raman spectra of water molecules vibration: deconvolution of OHs bands of Milli-Q water at 15 °C (a) and −15 °C (b). Raman spectra collected with different NaCl concentration (0.0, 10, 30, 50.0, 70.0 g/l): at 15 °C without sediments (c) and with sediments (d); at −15 °C without sediments (e) and with sediments (f).

Table 2
Raman shifts of pure water at 15 and −15 °C.

Band	15 °C Raman shift cm^{-1}	−15 °C Raman shift cm^{-1}
DDA-OH	3199.9	3132.6
DAA-OH	3392.3	3218.8
DA-OH	3530.1	3331.6
free OH	3614.7	3576.0

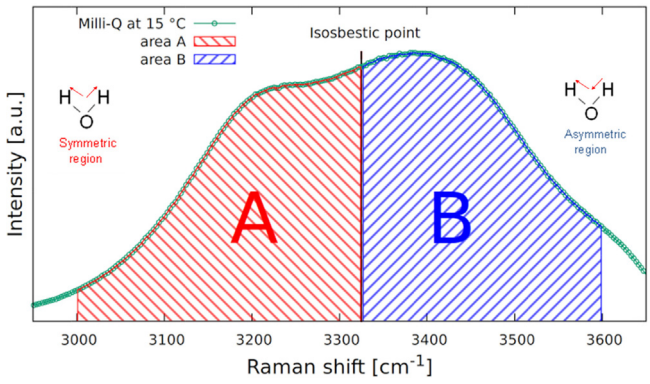

Fig. 7. Determination of the isosbestic point at 3325 cm^{-1} that divide the Raman spectrum of pure water at 15 °C in A and B regions.

Results showed in this section proved that the effect of sodium chloride and also the influence of sand particles on gas hydrate formation are function of temperature.

In the previous section, experiments were carried out below the ice-point and a different kind of relation was defined. At temperatures below the ice-point, the presence of sand was found to counteract the inhibiting effect of salt. Conversely, in these latter experiments, the influence of sand was proved, but its effect was found to be the opposite: above the ice-point, but below 3 – 5 °C, the presence of sand was found to contribute, together with salt, to inhibit hydrates formation. As expected, relevant differences were noticed between experiments carried out respectively below and above the freezing point of water. Below 0 °C, the formation of ice must be considered. This phenomenon is commonly considered disadvantageous for the production of hydrates,

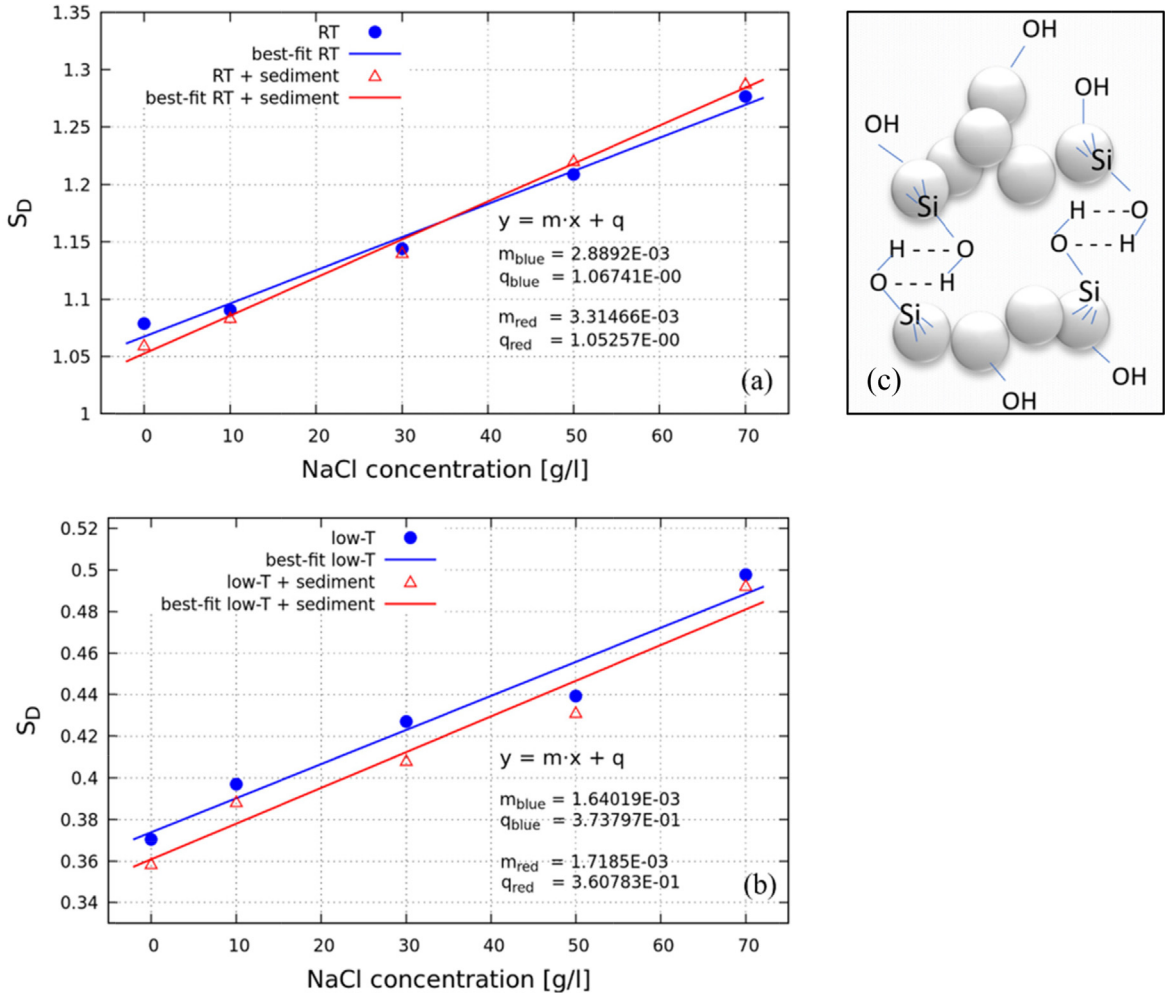

Fig. 8. Correlation of S_D concentration index at RT (15 °C) (a) and low-T (-15° C), with (red) and without sediment (blue) as a function of salinity (NaCl) (b). Schematic representation of interaction between silicate surface and water molecules (c). (For interpretation of the references to colour in this figure legend, the reader is referred to the web version of this article.)

Table 3
List of experiments described in section 3.2.2 and in section 3.3.3.

Salinity [g/l]	Methane	Carbon dioxide
0	A	D
30	B	E
37	C	F

because water molecules have the possibility to form a solid lattice and so reach a more ordered configuration, also in absence of guest compounds; thus, the formation of hydrates becomes slower and less massive, due to the competition with ice. However, when hydrates originate directly from ice crystal, they are obviously not affected by the inhibiting effect of sodium chloride. Thanks to the extremely favourable thermodynamic conditions, when hydrate clusters form from subcooled water (instead from ice), the presence of puckered and irregular surfaces, provided by sand grains, prevailed on the inhibiting effect of salt, and favoured anyway the formation of hydrates.

The variation with temperature proved that differences observed in the inhibiting action of sodium chloride are in a certain way correlated to the heat transfer rate of sand. This possibility was not unexpected: lots of chemical inhibitors were characterized in the past decades and lots of them were found to increase or reduce their inhibiting action as a function of temperature. For instance, Lee and colleagues [55] tested cyclic ethers, cyclic esters and cyclic ketone compounds. These substances are known for their high solubility in water. They asserted that 2-M−THF has a double effect on methane hydrates formation. While its action is negligible at temperatures close to 278 K, this compound is a promoter for the process at lower temperatures, while it acts as inhibitor at higher values. Ohmura et al. [62] studied methane hydrates formation in presence of 3-methyl-1-butanol. They observed that this additive favoured the process at temperatures below 279 K, while the opposite occurred for higher values. Jager and coworkers [63] proved that, at a specific temperature value the variation of 1,4-dioxane concentration in water could lead to inhibition or promotion of the process.

3.2.2. Experiments carried out with carbon dioxide as guest compound

In Fig. 9 d,e,f, a similar comparison was produced by using carbon dioxide as the guest compound. Experiments made with carbon dioxide led to the same conclusions asserted for methane hydrates. In the absence of sodium chloride, equilibrium conditions for CO_2 hydrates were extremely similar, but in the presence of sand, hydrates formed at milder conditions. The difference in temperature, when pressure is the same, is about 0.8 – 1.0 °C; conversely, pressure varied about 0.3 – 0.4 MPa at the same temperature.

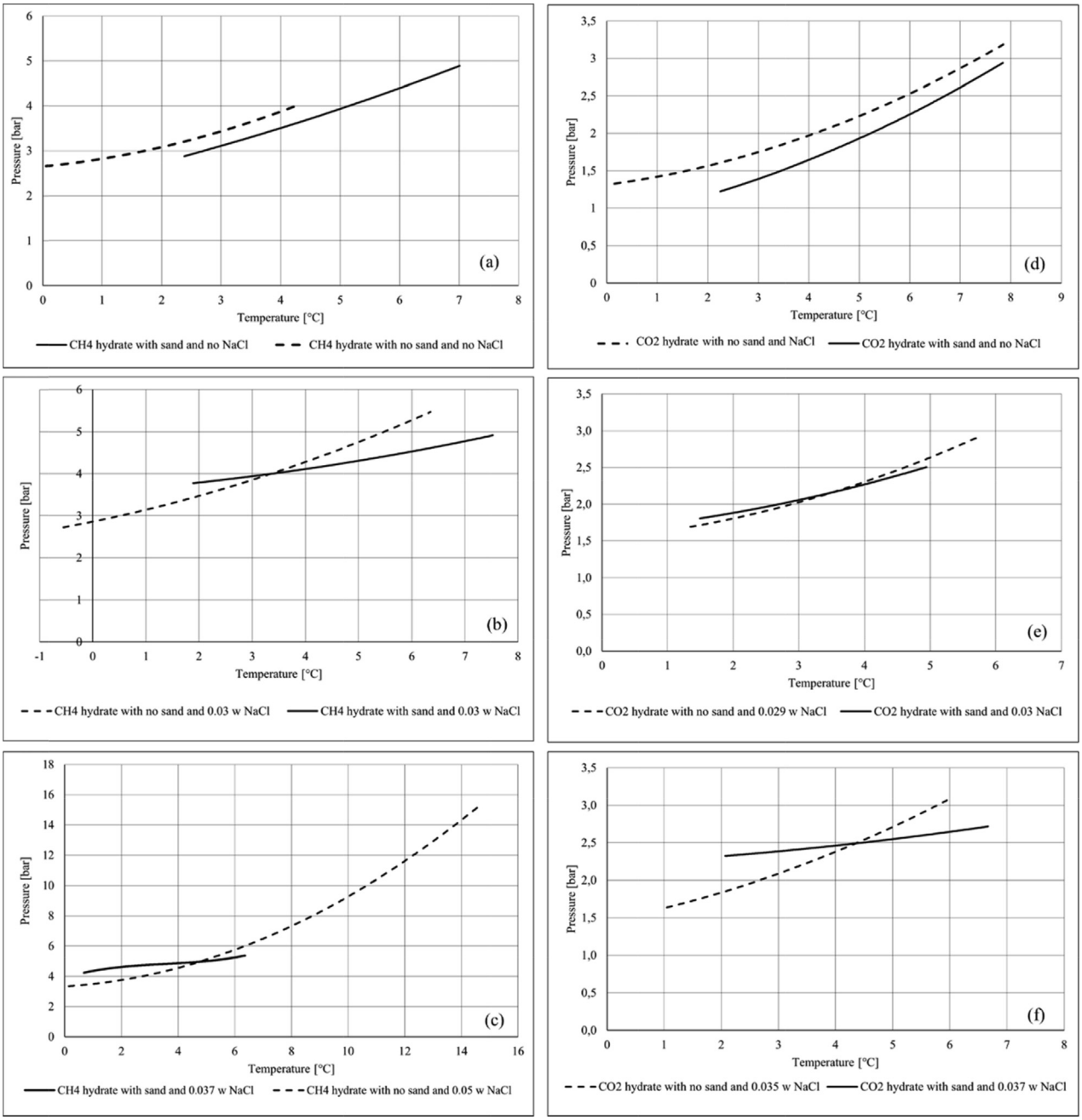

Fig. 9. Comparison between CH_4 and CO_2 hydrates equilibria; in pure demineralized water (a,d, respectively); in presence of NaCl (0.030 w) (b, e, respectively); in presence of NaCl (0.037 w) (c, f respectively); with sand (continuous line) and with no sand (dotted line).

The addition of salt also produced a similar trend: the two diagrams were not parallel anymore and an intersection point was found in the temperature range 3 – 5 °C. The only observed difference consists of the angle formed by the two curves, but further analyses would be needed to define its meaning with accuracy. However, this difference suggests that the effect of the contemporary presence of quartz sand and sodium chloride on the hydrate formation process may vary as a function of the type of guest compound involved in the process. In fact, this latter aspect would not represent a novelty: several examples are present in literature about chemical additives whose inhibiting action depends on properties of the guest compound.

For instance, the amino acid may provoke opposite kinetic effect, depending on the specific guest. Histidine was found to be a kinetic inhibitor for carbon dioxide hydrates [64] and, at the same time, it is a good kinetic promoter for methane hydrates [65,77]. Similarly, leucine is a well-known kinetic promoter for methane, while it inhibits THF-C_2H_6 hydrates [66]. Similar conclusions were also made for sodium chloride in previous works, where it was proved that the inhibition is stronger for methane than for carbon dioxide hydrates and such difference was also a function of the overall salinity degree [24,43,44].

4. Conclusions

The objective of this paper was to investigate, with both a micro-scale and macro-scale approach, the hydrate formation process and the interaction between sediment and salinity on it.

Since natural gas hydrates present similarity with the ice water and are generally formed in the condition where salinity, sediments, and temperature play an important role, in the first section of this study, we have monitored with Raman measurements the effect of these parameters on water hydrogen bond in liquid and ice phase conditions. Morphological information related to the sediment surface, by SEM measurements to the ice of pure water and to the ice in the presence of NaCl, were obtained to characterize the processes.

To clarify the effects of modification induced by the salt, sediments and temperature on water OH-stretching vibrations, different samples of ultrapure water and NaCl water solutions at different temperatures, were investigated by studying Raman spectra. Specific information on how the development of hydrogen bonds is influenced by the different conditions of the liquid and ice water phase were obtained and analyzed. Important differences in the OHs bands were observed with the variation of saline water concentration and temperature, and five components were determined by spectra deconvolution permitting a good description of these bands. Successively, two regions were identified in the range 3000–3600 cm^{-1}, each area measured and all SD indexes calculated. Specific equations were obtained when SD values were correlated with NaCl concentration in the liquid and ice water phase. An important observation was obtained in the presence of sediments, that is, in the ice phase, hydrophilic interaction with the silanol group of sediments produces a limitation of the salt effect.

From a macro-scale point of view, the hydrate dissociation/formation conditions of methane and carbon dioxide, in the presence of pure water, 0.030 and 0.037 wt% of NaCl solutions, were experimentally investigated. The second section of this work consisted of experiments about methane and carbon dioxide hydrates equilibrium.

We conducted experiments in solutions with and without sand in a lab-scaled reactor, filled with pure quartz porous sand. In order to observe and assess the inhibitor/promoter differences, the equilibrium curves of methane and carbon dioxide between literatures and experiments were compared for each salinity concentration in the temperature range of 0 – 8 °C. Results were then compared with data present in literature and related to the same typology of experiments carried out without sand. The present comparison proved that the presence of a porous medium generally promotes the hydrates formation process, as expected. Moreover, sand grains were also found to counteract the inhibiting effect of salt molecules, thus favoring hydrates formation at milder conditions than those described in the literature in the presence of similar concentrations of sodium chloride but without sand.

Results revealed that sand acted as the promoter for the process, independently by the presence of sodium chloride. It was also proved by comparing results described in this work with previous scientific research, where hydrates were formed in pure fresh water and without using a porous medium. In this latter case, pressure and temperature conditions were found to be extremely similar to equilibrium data present elsewhere in literature. Conversely, in this work, the presence of such porous medium favored hydrate formation at milder thermodynamic conditions than those usually required for the process completion. Such effect was mainly due to the higher values of surface/volume ratio and gas–liquid interface, reached in presence of sand; moreover, it also favored the heat transfer along the whole reactor.

Tests performed with salt (two different concentrations were tested: 0.03 w and 0.037 w) revealed that sand acted as a promoter at temperatures above 3 – 5 °C, while it inhibited the process for lower temperatures. The comparison between equilibrium diagrams produced with and without sand, clearly defines an intersection point in the temperature range.

Both types of experiments (microscopic measurements on ice and macroscopic measurements on gas hydrates) confirmed the influence exercised by sand on inhibiting effect of the sodium chloride during hydrates formation. Experiments on phase equilibrium boundaries suggested a relation between such variation and the heat transfer rate of the sediment; however, there are currently not enough information to assert it and further experiments are needed.

CRediT authorship contribution statement

Rita Giovannetti: Funding acquisition, Project administration, Conceptualization, Supervision, Writing – review & editing. **Alberto Maria Gambelli:** Conceptualization, Methodology, Formal analysis, Data curation, Writing – review & editing. **Beatrice Castellani:** Conceptualization, Methodology, Writing – review & editing. **Andrea Rossi:** Methodology, Formal analysis, Data curation. **Marco Minicucci:** Methodology, Formal analysis, Data curation. **Marco Zannotti:** Methodology, Formal analysis, Data curation. **Yan Li:** Conceptualization, Writing – review & editing. **Federico Rossi:** Funding acquisition, Project administration, Supervision.

Declaration of Competing Interest

The authors declare that they have no known competing financial interests or personal relationships that could have appeared to influence the work reported in this paper.

Acknowledgements

The authors gratefully acknowledge financial support derived from MIUR by the PRIN Project 2017 entitled: "Methane recovery and carbon dioxide disposal in natural gas hydrate reservoirs" Prot.20173K5L3K. The authors gratefully acknowledge the School of Science of and Technology of University of Camerino for providing important technical and scientific resources such as the field-emission SEM (Sigma 300) and the customized micro-Raman spectroscopy equipment (Olympus-Horiba iHR320), necessary for this work.

References

[1] E.D. Sloan, C.A. Khon, Clathrate Hydrates of Natural Gases, third edition ed., CRC Press, 2007. 978-0849390784.
[2] R.K. McMullan, G.A. Jeffrey, Polyhedral clathrate hydrates. IX. Structure of ethylene oxide hydrate, J. Chem. Phys. 42 (8) (1965) 2725–2732.
[3] K.V. Kumar, K. Preuss, M.-M. Titirici, F. Rodríguez-Reinoso, Nanoporous Materials for the Onboard Storage of Natural Gas, Chem. Rev. 117 (2017) 1796–1825, https://doi.org/10.1021/acs.chemrev.6b00505.
[4] X.-S. Li, C.-G. Xu, Y.u. Zhang, X.-K. Ruan, G. Li, Y.i. Wang, Investigation into gas production from natural gas hydrate: A review, Appl. Energy 172 (2016) 286–322.
[5] Y.F. Makogon, Natural gas hydrates – A promising source of energy, J. Nat. Gas Sci. Eng. 2 (1) (2010) 49–59.
[6] M.D. Max, Natural gas hydrate in oceanic and permafrost environments, Springer, 2003.
[7] R. Boswell, T.S. Collett, Current perspectives on gas hydrate resources, Energy Environ. Sci. 4 (4) (2011) 1206–1215, https://doi.org/10.1039/C0EE00203H.
[8] T.S. Collett, A.H. Johnson, C.C. Knapp, R. Boswell, Natural Gas Hydrates: A Review, in: T. Collett, A. Johnson, C. Knapp, R. Boswell (eds.) Natural Gas Hydrates—Energy Resource Potential and Associated Geologic Hazards, Vol. 89, American Association of Petroleum Geologists, 2009.
[9] A. Hassanpouryouzband, E. Joonaki, M. Vasheghani Farahani, S. Takeya, C. Ruppel, J. Yang, N.J. English, J.M. Schicks, K. Edlmann, H. Mehrabian, Z.M. Aman, B. Tohidi, Gas hydrates in sustainable chemistry, Chem. Soc. Rev. 49 (15) (2020) 5225–5309.
[10] L. Jiang, M. Yu, Y.u. Liu, M. Yang, Y.i. Zhang, Z. Xue, T. Suekane, Y. Song, Behavior of CO2/water flow in porous media for CO2 geological storage, Magn. Reson. Imaging 37 (2017) 100–106.
[11] S. Merey, R.I. Al-Raoush, J. Jung, K.A. Alshibli, Comprehensive literature review on CH4-CO2 replacement in microscale porous media, J. Petroleum Sci. Eng. 171 (2018) 48–62.

[12] O. Ors, C. Sinayuc, An experimental study on the CO2–CH4 swap process between gaseous CO2 and CH4 hydrate in porous media, J. Petroleum Sci. Eng. 119 (2014) 156–162, https://doi.org/10.1016/j.petrol.2014.05.003.
[13] P. Wang, M. Yang, B. Chen, Y. Zhao, J. Zhao, Y. Song, Methane hydrate reformation in porous media with methane migration, Chem. Eng. Sci. 168 (2017) 344–351.
[14] J. Zhao, Z. Zhu, Y. Song, W. Liu, Y.i. Zhang, D. Wang, Analyzing the process of gas production for natural gas hydrate using depressurization, Appl. Energy 142 (2015) 125–134.
[15] A.M. Gambelli, U. Tinivella, R. Giovannetti, B. Castellani, M. Giustiniani, A. Rossi, M. Zannotti, F. Rossi, Observation of the Main Natural Parameters Influencing the Formation of Gas Hydrates, Energies 14 (2021) 1803, https://doi.org/10.3390/en14071803.
[16] P.D. Dholabhai, N. Kalogerakis, P.R. Bishnoi, Equilibrium conditions for carbon dioxide hydrate formation in aqueous electrolyte solutions, J. Chem. Eng. Data 38 (4) (1993) 650–654, https://doi.org/10.1021/je00012a045.
[17] M. Cha, Y. Hu, A.K. Sum, Methane hydrate phase equilibria for systems containing NaCl, KCl, and NH4Cl, Fluid Phase Equilib. 413 (2016) 2–9.
[18] H. Mimachi, S. Takeya, Y. Gotoh, A. Yoneyama, K. Hyodo, T. Takeda, T. Murayama, Dissociation behaviors of methane hydrate formed from NaCl solutions, Fluid Phase Equilib. 413 (2016) 22–27.
[19] S. Ho-Van, B. Bouillot, J. Douzet, S.M. Babakhani, J.M. Herri, Cyclopentane hydrates – A candidate for desalination?, Journal of Environmental, Chem. Eng. 7 (5) (2019) 103359, https://doi.org/10.1016/j.jece:2019.103359.
[20] P. Babu, A. Nambiar, T. He, I.A. Karimi, J.D. Lee, P. Englezos, P. Linga, A Review of Clathrate Hydrate Based Desalination To Strengthen Energy-Water Nexus, ACS Sustainable Chem. Eng. 6 (7) (2018) 8093–8107, https://doi.org/10.1021/acssuschemeng.8b01616.
[21] M. Inui, A. Ando, H. Kagemoto, T. Komai, Y. Sakamoto, T. Kawamura, Behavior of Gas Hydrate Formation In Marine Sediments For CO2 Sequestration, in, 2005.
[22] P. Thoutam, S. Rezaei Gomari, A. Chapoy, F. Ahmad, M. Islam, Study on CO2 Hydrate Formation Kinetics in Saline Water in the Presence of Low Concentrations of CH4, ACS Omega 4 (19) (2019) 18210–18218.
[23] T. Nakashima, T. Sato, M. Inui, Numerical Modeling of Hydrate Formation in Sand Sediment Simulating Sub-Seabed CO2 Storage in the form of Gas Hydrate, Energy Procedia 37 (2013) 5986–5993.
[24] A.M. Gambelli, B. Castellani, A. Nicolini, F. Rossi, Water Salinity as Potential Aid for Improving the Carbon Dioxide Replacement Process' Effectiveness in Natural Gas Hydrate Reservoirs, Processes 8 (10) (2020) 1298, https://doi.org/10.3390/pr8101298.
[25] M.J. Castaldi, Y. Zhou, T.M. Yegulalp, Down-hole combustion method for gas production from methane hydrates, J. Petroleum Sci. Eng. 56 (1-3) (2007) 176–185.
[26] S. Takeya, J. Ripmeester, Dissociation Behavior of Clathrate Hydrates to Ice and Dependence on Guest Molecules, Angew. Chem. Int. Ed. 47 (7) (2008) 1276–1279.
[27] P.S.R. Prasad, V.D. Chari, Preservation of methane gas in the form of hydrates: Use of mixed hydrates, J. Nat. Gas Sci. Eng. 25 (2015) 10–14.
[28] G.A. Jeffrey, W. Saenger, Hydrogen-Bonding Patterns in Water, Ices, the Hydrate Inclusion Compounds, and the Hydrate Layer Structures, in: G.A. Jeffrey, W. Saenger (eds.) Hydrogen Bonding in Biological Structures, Springer Berlin Heidelberg, Berlin, Heidelberg, 1991, pp. 425-451.
[29] M.A. Ahmadi, A. Bahadori, Chapter Eight - Gas Hydrates, in: A. Bahadori (ed.) Fluid Phase Behavior for Conventional and Unconventional Oil and Gas Reservoirs, Gulf Professional Publishing, Boston, 2017, pp. 405-444.
[30] C. Holzammer, J.M. Schicks, S. Will, A.S. Braeuer, Influence of Sodium Chloride on the Formation and Dissociation Behavior of CO2 Gas Hydrates, J. Phys. Chem. B 121 (2017) 8330–8337, https://doi.org/10.1021/acs.jpcb.7b05411.
[31] C.A. Koh, R.E. Westacott, W. Zhang, K. Hirachand, J.L. Creek, A.K. Soper, Mechanisms of gas hydrate formation and inhibition, Fluid Phase Equilib. 194-197 (2002) 143–151.
[32] J. Du, L. Jiang, Q.i. Shao, X. Liu, R.S. Marks, J. Ma, X. Chen, Colorimetric Detection of Mercury Ions Based on Plasmonic Nanoparticles, Small 9 (9-10) (2013) 1467–1481.
[33] E.G. Hammerschmidt, Formation of Gas Hydrates in Natural Gas Transmission Lines, Ind. Eng. Chem. 26 (1934) 851–855, https://doi.org/10.1021/ie50296a010.
[34] W.M. Deaton, J.E.M. Frost, Gas hydrates and their relation to the operation of natural-gas pipe lines, in, United States (1946).
[35] J.L. De Roo, C.J. Peters, R.N. Lichtenthaler, G.A.M. Diepen, Occurrence of methane hydrate in saturated and unsaturated solutions of sodium chloride and water in dependence of temperature and pressure, AIChE J. 29 (4) (1983) 651–657.
[36] A.H. Mohammadi, W. Afzal, D. Richon, Gas hydrates of methane, ethane, propane, and carbon dioxide in the presence of single NaCl, KCl, and CaCl2 aqueous solutions: Experimental measurements and predictions of dissociation conditions, J. Chem. Thermodyn. 40 (12) (2008) 1693–1697.
[37] F. Rossi, A.M. Gambelli, Thermodynamic phase equilibrium of single-guest hydrate and formation data of hydrate in presence of chemical additives: a review, Fluid Phase Equilib. 536 (2021) 112958, https://doi.org/10.1016/j.fluid.2021.112958.
[38] J.G. Vlahakis, The Growth Rate of Ice Crystals: the Properties of Carbon Dioxide Hydrate, a Review of Properties of 51 Gas Hydrates, U.S. Department of the Interior, 1972.
[39] L.i. Zha, D.-Q. Liang, D.-L. Li, Phase equilibria of CO2 hydrate in NaCl–MgCl2 aqueous solutions, J. Chem. Thermodyn. 55 (2012) 110–114.
[40] S.-C. Sun, C.-L. Liu, Y.-G. Ye, Phase equilibrium condition of marine carbon dioxide hydrate, J. Chem. Thermodyn. 57 (2013) 256–260.
[41] C.C. Holzammer, A.S. Braeuer, Raman Spectroscopic Study of the Effect of Aqueous Salt Solutions on the Inhibition of Carbon Dioxide Gas Hydrates, J. Phys. Chem. B 123 (2019) 2354–2361, https://doi.org/10.1021/acs.jpcb.8b11040.
[42] K. Nasrifar, M. Moshfeghian, A model for prediction of gas hydrate formation conditions in aqueous solutions containing electrolytes and/or alcohol, J. Chem. Thermodyn. 33 (9) (2001) 999–1014.
[43] A.M. Gambelli, F. Rossi, The use of sodium chloride as strategy for improving CO2/CH4 replacement in natural gas hydrates promoted with depressurization methods, Arabian J. Geosci. 13 (2020) 898, https://doi.org/10.1007/s12517-020-05879-6.
[44] A.M. Gambelli, M. Filipponi, F. Rossi, Natural gas hydrate: effect of sodium chloride on the CO2 replacement process, in: 19th International Multidisciplinary Scientific GeoConference SGEM 2019, Sofia, 2019, pp. 333-344.
[45] A.M. Gambelli, An experimental description of the double positive effect of CO2 injection in methane hydrate deposits in terms of climate change mitigation, Chem. Eng. Sci. 233 (2021) 116430, https://doi.org/10.1016/j.ces.2020.116430.
[46] A.M. Gambelli, F. Rossi, Thermodynamic and kinetic characterization of methane hydrate 'nucleation, growth and dissociation processes, according to the Labile Cluster Theory, Chem. Eng. J. 425 (2021) 130706, https://doi.org/10.1016/j.cej.2021.130706.
[47] R. Anderson, M. Llamedo, B. Tohidi, R.W. Burgass, Experimental Measurement of Methane and Carbon Dioxide Clathrate Hydrate Equilibria in Mesoporous Silica, J. Phys. Chem. B 107 (2003) 3507–3514, https://doi.org/10.1021/jp0263370.
[48] R. Anderson, M. Llamedo, B. Tohidi, R.W. Burgass, Characteristics of Clathrate Hydrate Equilibria in Mesopores and Interpretation of Experimental Data, J. Phys. Chem. B 107 (2003) 3500–3506, https://doi.org/10.1021/jp0263368.
[49] S.-P. Kang, J.-W. Lee, H.-J. Ryu, Phase behavior of methane and carbon dioxide hydrates in meso- and macro-sized porous media, Fluid Phase Equilib. 274 (1-2) (2008) 68–72.
[50] Y.P. Handa, D.Y. Stupin, Thermodynamic properties and dissociation characteristics of methane and propane hydrates in 70-.ANG.-radius silica gel pores, The Journal of Physical Chemistry, 96 (1992) 8599-8603.10.1021/j100200a071.
[51] O. Nashed, B. Partoon, B. Lal, K.M. Sabil, A.M. Shariff, Review the impact of nanoparticles on the thermodynamics and kinetics of gas hydrate formation, J. Nat. Gas Sci. Eng. 55 (2018) 452–465.
[52] A. Nurulhuda, S. Yusup, M.S. Khalik, CO2 Sequestration on Porous Media with Presence of Water: A review, in: 27th International Symposium on Chemical Engineering, Kuala Lampur, Malaysia, 2014.
[53] Z.R. Chong, A.H.M. Chan, P. Babu, M. Yang, P. Linga, Effect of NaCl on methane hydrate formation and dissociation in porous media, J. Nat. Gas Sci. Eng. 27 (2015) 178–189.
[54] S.H.B. Yang, P. Babu, S.F.S. Chua, P. Linga, Carbon dioxide hydrate kinetics in porous media with and without salts, Appl. Energy 162 (2016) 1131–1140.
[55] J.-W. Lee, H. Lu, I.L. Moudrakovski, C.I. Ratcliffe, J.A. Ripmeester, Thermodynamic and Molecular-Scale Analysis of New Systems of Water-Soluble Hydrate Formers + CH4, J. Phys. Chem. B 114 (2010) 13393–13398, https://doi.org/10.1021/jp106466s.
[56] D.M. Carey, G.M. Korenowski, Measurement of the Raman spectrum of liquid water, J. Chem. Phys. 108 (1998) 2669–2675, https://doi.org/10.1063/1.475659.
[57] W.B. Monosmith, G.E. Walrafen, Temperature dependence of the Raman OH-stretching overtone from liquid water, J. Chem. Phys. 81 (1984) 669–674, https://doi.org/10.1063/1.447748.
[58] T. Shimoaka, T. Hasegawa, K. Ohno, Y. Katsumoto, Correlation between the local OH stretching vibration wavenumber and the hydrogen bonding pattern of water in a condensed phase: Quantum chemical approach to analyze the broad OH band, J. Mol. Struct. 1029 (2012) 209–216.
[59] K. Ohgaki, Y. Makihara, K. Takano, Formation of CO₂ Hydrate in Pure and Sea Waters, J. Chem. Eng. Jpn. 26 (1993) 558–564, https://doi.org/10.1252/jcej.26.558.
[60] D. Kyung, K. Lee, H. Kim, W. Lee, Effect of marine environmental factors on the phase equilibrium of CO2 hydrate, Int. J. Greenhouse Gas Control 20 (2014) 285–292.
[61] J.G. Speight, Chapter 4 - Hydrocarbons from natural gas and natural gas hydrates, in: J.G. Speight (Ed.), Handbook of Industrial Hydrocarbon Processes (Second Edition), Gulf Professional Publishing, Boston, 2020, pp. 143–192.
[62] R. Ohmura, S. Takeya, T. Uchida, I.Y. Ikeda, T. Ebinuma, H. Narita, Clathrate hydrate formation in the system methane + 3-methyl-1-butanol + water: equilibrium data and crystallographic structures of hydrates, Fluid Phase Equilib. 221 (1-2) (2004) 151–156.
[63] M.D. Jager, R.M. de Deugd, C.J. Peters, J. de Swaan Arons, E.D. Sloan, Experimental determination and modeling of structure II hydrates in mixtures of methane+water+1,4-dioxane, Fluid Phase Equilib. 165 (2) (1999) 209–223.
[64] J.-H. Sa, G.-H. Kwak, K. Han, D. Ahn, K.-H. Lee, Gas hydrate inhibition by perturbation of liquid water structure, Sci. Rep. 5 (2015) 11526, https://doi.org/10.1038/srep11526.

[65] G. Bhattacharjee, N. Choudhary, A. Kumar, S. Chakrabarty, R. Kumar, Effect of the amino acid l-histidine on methane hydrate growth kinetics, J. Nat. Gas Sci. Eng. 35 (2016) 1453–1462.
[66] Q. Sun, The Raman OH stretching bands of liquid water, Vib. Spectrosc. 51 (2) (2009) 213–217.
[67] Q. Sun, H. Zheng, Raman OH stretching vibration of ice Ih, Prog. Nat. Sci. 19 (11) (2009) 1651–1654.
[68] D.A. Schmidt, K. Miki, Structural Correlations in Liquid Water: A New Interpretation of IR Spectroscopy, J. Phys. Chem. A 111 (2007) 10119–10122, https://doi.org/10.1021/jp074737n.
[69] R. Mancinelli, A. Botti, F. Bruni, M.A. Ricci, A.K. Soper, Perturbation of water structure due to monovalent ions in solution, PCCP 9 (2007) 2959–2967, https://doi.org/10.1039/B701855J.
[70] P. Jungwirth, D.J. Tobias, Specific Ion Effects at the Air/Water Interface, Chem. Rev. 106 (4) (2006) 1259–1281, https://doi.org/10.1021/cr0403741.
[71] L. Vrbka, M. Mucha, B. Minofar, P. Jungwirth, E.C. Brown, D.J. Tobias, Propensity of soft ions for the air/water interface, Curr. Opin. Colloid Interface Sci. 9 (1-2) (2004) 67–73.
[72] I. Đuričković, M. Marchetti, R. Claverie, P. Bourson, J.-M. Chassot, M.D. Fontana, Experimental Study of NaCl Aqueous Solutions by Raman Spectroscopy: Towards a New Optical Sensor, Appl. Spectrosc. 64 (8) (2010) 853–857.
[73] F. Li, Z. Li, Y. Wang, S. Wang, X. Wang, C. Sun, Z. Men, A Raman spectroscopy study on the effects of intermolecular hydrogen bonding on water molecules absorbed by borosilicate glass surface, Spectrochim. Acta Part A Mol. Biomol. Spectrosc. 196 (2018) 317–322.
[74] A.M. Gambelli, Analyses on CH4 and CO2 hydrate formation to define the optimal pressure for CO2 injection to maximize the replacement efficiency into natural gas hydrate in presence of a silica-based natural porous medium, via depressurization techniques, Chem. Eng. Processing - Process Intensification 167 (2021) 108512, https://doi.org/10.1016/j.cep.2021.108512.
[75] M.S. Selim, E.D. Sloan, Heat and mass transfer during the dissociation of hydrates in porous media, AIChE J. 35 (6) (1989) 1049–1052.
[76] J.W. Ullerich, M.S. Selim, E.D. Sloan, Theory and measurement of hydrate dissociation, AIChE J. 33 (5) (1987) 747–752.
[77] Y. Liu, B. Chen, Y. Chen, S. Zhang, W. Guo, Y. Cai, B. Tan, W. Wang, Methane Storage in a Hydrated Form as Promoted by Leucines for Possible Application to Natural Gas Transportation and Storage, Energy Technology 3 (8) (2015) 815–819.